

446. Fellenius, B.H., Budge A.S., Dasenbrock D.D., Olson S.J. and Reuter G.R., 2026. Long-term monitoring of a pile abutment for force and settlement. Proceedings of the ICE, Geotechnical. Engineering, 179(5) 11 p. doi.org/10.1680/jgeen.25.00259

Cite this article
Fellenius BH, Budge AS, Dasenbrock DD, Olson SJ and Reuter GR
Long-term monitoring of a pile abutment for force and settlement.
Proceedings of the Institution of Civil Engineers – Geotechnical Engineering,
https://doi.org/10.1680/jgeen.25.00259

Research Article
Paper 2500259
Received 22/12/2025; Accepted 21/05/2026

Emerald Publishing Limited: All rights reserved

Geotechnical Engineering

Long-term monitoring of a pile abutment for force and settlement

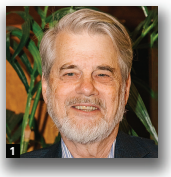
1 **Bengt H. Fellenius**
Consulting engineer, Sidney, BC, Canada (Orcid:0009-0009-3804-4301)
(corresponding author: bengt@fellenius.net)

2 **Aaron S. Budge**
Minnesota State University, Mankato, MN, USA

3 **Derrick D. Dasenbrock**
Minnesota Department of Transportation, Maplewood, MN, USA

4 **Steven J. Olson**
Kiewit Engineering Group Inc., Lenexa, KS, USA

5 **Gregory R. Reuter**
American Engineering Testing, Inc., St. Paul, MN, USA







The soil profile at the 1960 Eisenhower Bridge consisted of 10 m of loose sand and 15 m of soft, compressible clay overlying dense sand and gravel on sandstone. The bridge suffered drag force that exceeded the structural strength of the foundation wood piles, which effectively removed pile bearing and caused the piles to be dragged down by long-term soil settlement. Eventually, the bridge was replaced. Wick drains were installed for the replacement bridge embankments to accelerate settlements and pore pressure dissipation. Settlement, pore pressures and pile axial forces were monitored during and after construction. The piles terminating in the sand were found to carry a smaller load than piles terminating in the sandstone. An equilibrium plane developed that was deeper for the piles terminating on the sandstone. The consolidation of the clay layer took almost a full year. The new approach embankment settled about 400 mm, while the new H-piles settled only due to elastic compression and a small toe penetration. The development of drag force, downdrag and pile settlement was analysed according to the method expressed in the recently proposed revision of the American Association of State Highway and Transportation Officials (AASHTO) specifications.

Keywords: downdrag/drag force/foundations/geotechnical engineering/long-term monitoring/piled foundation/pore pressures/settlement/soft clay/strain-gauge instrumentation/stress analysis/wick drains

1. Introduction

That soil settling around a pile will transfer force, drag force, to the pile was first measured in the 1960s (Bjerrum *et al*., 1969; Endo *et al*., 1969; Fellenius and Broms, 1969; Johannessen and Bjerrum, 1965; Okabe, 1977). The understanding that the key issue is the downdrag rather than the drag force came later, in 2006 (Bartz and Blatz, 2020; Coffman *et al*., 2024a; Fellenius, 1984, 1988, 2006; Siegel, 2025).

Bridges incorporate embankment fills and are often constructed in regions with compressible soil resulting in settlement and associated negative skin friction, drag force and downdrag caused, in particular, by the approach embankment. The downdrag can introduce significant differential settlement between the abutment structure and the approach embankment. In about 2010, to enhance background knowledge for the design of piled foundations for bridges, the Minnesota Department of Transportation (MnDOT) implemented monitoring of piled foundations, supporting bridges in the Mississippi River valley, where soil and site conditions implied downdrag issues due to the presence of thick layers of soft silty clay, organic matter and calcareous materials within sandy soil deposits overlying the bearing soil layers. One such project was the bridge replacing the Eisenhower Bridge across the Mississippi River. The old bridge was built in 1960 to connect Red Wing, Minnesota, to Hager City, Wisconsin. It was supported on timber piles and, over time, the abutment and embankment settled. A 1984 maintenance report documented that the embankment had settled more than 1.2 m (3.9 ft) since its construction in 1961. Construction of the significantly widened 500 m (1640 ft) replacement bridge started in 2017. The new bridge's south embankment was supported on ground, but the north abutment was supported on H-piles; drilled shafts were used to support the main span at piers 1 and 2. The pile forces and soil settlement at the north abutment were monitored at the start of construction and this was continued until about 2 years after construction.

2. Soil profile

From the ground surface at about an elevation of +207 m (+680 ft), the soil profile at the bridge site consisted of an approximately 10 m (35 ft) thick, very loose, silty sand layer including

some fill, underlain by about 15 m (50 ft) of soft, normally consolidated, compressible very soft to soft, organic to highly organic silty clay. Results of oedometer tests indicated that the compressibility of the soft clay was $C_c = 0.4$ and $e_0 = 1.50$, correlating to a Janbu modulus number (m) of 9, which indicates a very compressible soil ($m < 10$). The soil is normally consolidated and the coefficient of consolidation, c_v, was reported to be about 4 m^2/year (40 ft^2/year).

The clay is underlain by an approximately 15 m (50 ft) thick deposit of very dense sand and gravel. At a depth of about 25 m (80 ft), the soil profile changes to a 3 m (10 ft) thick layer of dense to very dense sand and gravel followed by compact coarse sand above cemented sand (sandstone) at a depth of 42 m (138 ft).

The groundwater table in the sand layer was affected by the water level in the river, which seasonally fluctuated by as much as about 5 m (15 ft). The normal river level was at elev. +203 m (+666 ft), that is about 4.3 m (14 ft) below the ground surface at the abutment. The pore pressure in and below the clay layer is assumed to fluctuate relatively less. At the bridge abutment foundation, the water table from pore pressures in the clay would be at about 0.6 m (2 ft) depth.

Figure 1 shows the cone penetration test (CPT) diagrams from two CPT soundings pushed from about elev. +207 m (+680 ft) near the abutment, one at each side of the new embankment. The soundings showed that the soil above the very dense sand and gravel was very loose/very soft.

Figure 2 shows the N-indices from two standard penetration test (SPT) borings with the two CPT q_c diagrams added. The label 'Pz' identifies the depths of the piezometers of the piezometer stations placed at the new bridge in October 2017.

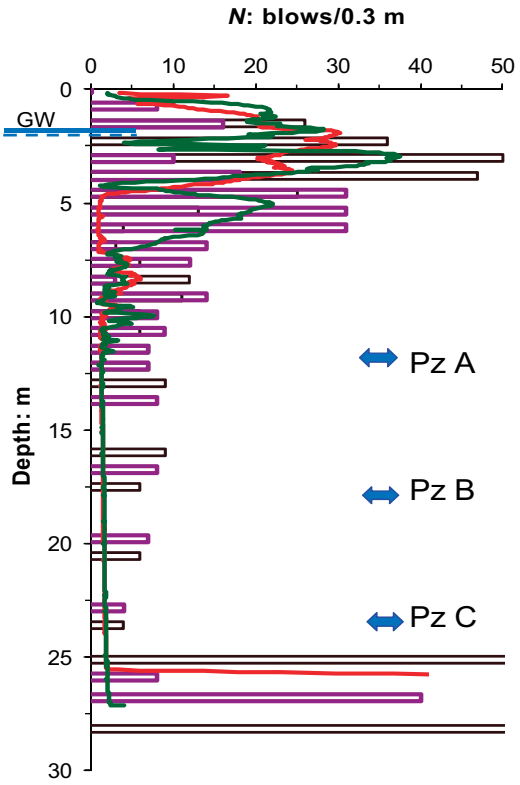


Figure 2. Standard penetration test (SPT) N-indices from two boreholes with two CPT sounding (q_t) diagrams and piezometer depths

3. The old Eisenhower Bridge

The conditions and observations at the old Eisenhower Bridge were compiled by Olson (2020). The highest original ground surface at

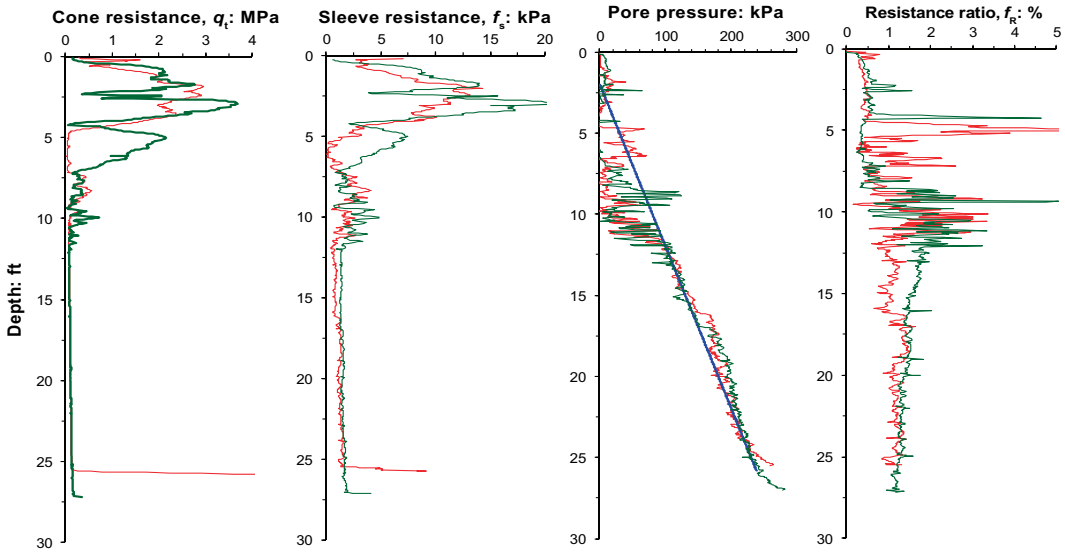


Figure 1. Cone penetration test (CPT) diagram from two CPT soundings at the north embankment

the north abutment of the bridge was at elev. +207.3 m (+680 ft). The final elevation of the north abutment's road surface was elev.+211.8 m (+695 ft), about 5 m (15 ft) above the highest level of the original ground. The abutment was placed on 26 timber piles, with a cut-off elevation at elev. +210.3 m (+690 ft). The average pile length below cut-off was 29.5 m (97 ft) and the pile toe was at elev. +180.7 m (+593 ft), that is the pile toes were on average about 0.6 m (2 ft) into the very dense sand and gravel layer.

The pile head and toe diameters were about 380 mm (15 in) and 180 mm (7 in), respectively. The piles were driven to an average termination resistance of 2 mm/bl (0.08 in/bl). The sustained load was close to 180 kN/pile (40 kips/pile). The compressive strength of the timber piles was indicated to be 8.6 MN (1.25 ksi). At the upper and lower boundaries of the clay layer, the proportional pile diameters were 280 mm and 180 mm, respectively (11 and 7 in, respectively) and the corresponding axial compressive strengths amounted to about 530 kN (120 kips) and 220 kN (50 kips), respectively.

No formal monitoring of the old bridge was implemented. However, over time, it was noticed that the pile-supported bridge abutment and the approach embankment both settled by the same amount; about 'several feet' (Olson, 2020).

Figure 3 shows the distribution of force and settlement for the timber piles as per the unified method (Coffman *et al*., 2024a; Fellenius, 1984, 2026). Figure 3(a) shows the assumed force distribution for the 7.6 m (25 ft) high embankment as indicated by Olson (2020). Figure 3(b) shows the settlement distribution of the soil and the bridge piles calculated using the reported compressibilities of the clay, sand and gravel. Figure 3(a) shows the force distribution of a 'strong pile', which would develop an equilibrium (equilibrium plane (EP) (Fellenius, 2025)) between the sustained bridge load plus drag force and shaft resistance and toe force at the lower boundary of the clay layer, if the pile axial strength could be assumed to be larger than the maximum force in the pile developing at the EP. However, the actual, structural axial strength of the wood pile in the clay is smaller than the indicated axial force. The red line denotes the pile axial strength, correlated to the depth-reducing pile diameter of the timber pile. The blue line shows the increase of axial force due to the drag force. When the two lines intersect, the force exceeds the strength and the pile breaks. That the timber pile would have been able to sustain the maximum axial force and develop the toe resistance of about 500 kN (100 kips) indicated in the figure is unlikely. Before the substantial downdrag would have been able to push the actual pile toe to that mobilised resistance, the pile would have broken (splintered; sheared off) somewhere above 20 m (65 ft) depth. The pile toe of the 'new' shorter pile would only be able to mobilise a small toe resistance. Therefore, a new EP would have developed at about 7 m (23 ft) depth and the pile head settlement, as shown in Figure 3(b), would have become about equal with the ground surface, which is what the records also indicate. The timber piles settled equally with the embankment. This is likely to be because the piles broke as a result of their being overstressed by the drag force.

Normally, the issue of soil settling around a pile concerns the downdrag. This is a first documentation of a case where the drag force was the decisive factor for the damage to the piles and the problem for the piled foundation. Had the piles been steel piles or concrete piles and driven to achieve sufficient toe bearing, ensuring a small long-term pile-toe movement, the piles would not have broken. However, the embankment would have experienced significant settlement, and frequent and costly maintenance to restore the vertical alignment between the bridge deck and the approach embankment would have been necessary.

4. The new Eisenhower Bridge

As reported by Dasenbrock *et al*. (2021) and Dasenbrock and Chow (2023), the replacement bridge was constructed alongside the old bridge and the use of the old bridge was maintained until the

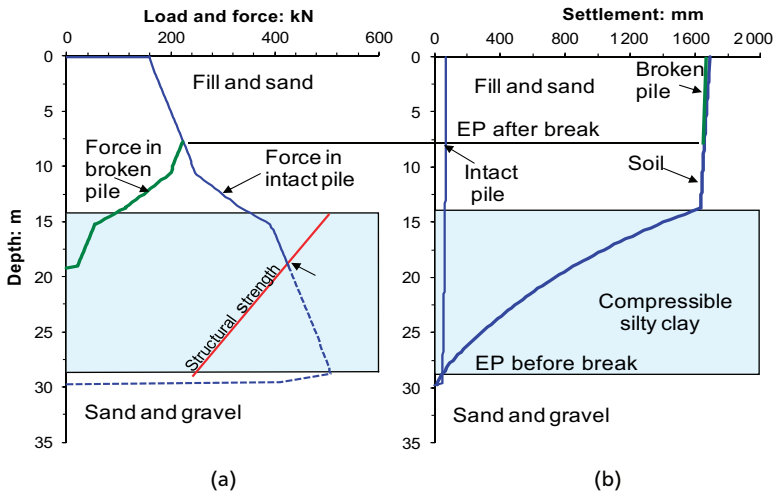


Figure 3. Distributions of (a) load and force and (b) settlement

new bridge was completed. The north approach abutment of the new bridge was taller and wider than for the old bridge. The width was 21 m (70 ft) and the sides sloped 1(V):3(H). The approach embankment surface at the abutment was at elev.+214.9 m (+705 ft), about 8 m (25 ft) above the highest ground surface level of about elev.+207.2 m (+680 ft) – approximately the same as at the old bridge. The pile abutment was supported on H-piles driven on 28 July 2017, set as 'day zero' for the monitoring.

To reduce the settlement of the embankment after construction and paving, between 26 September 2017 and 25 October 2017 (days 60 through 90 after pile driving), wick drains were installed to the lower boundary of the compressible soil, about elev.+182.9 m (+600 ft). The drains were of type Amerdrain 407, with 100 mm (4 in) wide continuous corrugated polypropylene core wrapped in a polypropylene geotextile filter. They were installed at 1.5 m (5 ft) spacing in a triangular grid behind the abutment over a 21 m (70 ft) wide and 150 m (500 ft) long area. Some embankment fill was placed concurrent with the drain installation, but the main construction of the embankment occurred in April and June 2018, on days 300 and 430, when about 5 m (16 ft) and 3.0 m (10 ft) embankment fill and surcharge were placed. The bridge beam and pile cap were poured on day 390 and the bridge deck was poured on day 450.

4.1 Piles

The new bridge is supported on 18 14HP117 piles with a cut-off level at elev.+204.0 m (+687 ft). The piles were driven from a working platform at least 2 m (7 ft) above the original ground in the newly placed widened embankment.

The pile cross-sectional area (steel) was 222 cm^2 (34.4 in^2) and the area of the circumscribing rectangle was 1356 cm^2 (210 in^2). The circumference of the rectangle was 1.5 m (4.9 ft). Steel yield strength was 345 MPa (50 ksi). With a steel E modulus of 207 GPa (30 000 ksi), the EA parameter was 4.7 GN (1.05×10^6 kips).

The abutment pier footing was 17.4 × 4.3 m (57 × 14 ft) and the piles were placed in three rows. Figure 4 shows the layout of the footing and test piles. The pile centre-to-centre spacing was 3.2 m (10.6 ft) east to west and 1.5 m (5 ft) north to south. The piles were driven in 15 m (50 ft) sections by a Delmag D46-32 single-acting diesel hammer, using fuel setting 4. All but one pile, pile TP2, of the 18 abutment production piles were terminated in the sandstone bedrock, as indicated by the pile penetration resistance at a depth of 43 m (142 ft) and, thus, the length below cut-off was 45 m (149 ft). Pile TP2 was terminated 1.5 m (5 ft) higher in the very dense sand and gravel at 41.8 m (137 ft) final depth. The length below cut-off was 43.9 m (144 ft). Two additional piles with the same cut-off level, piles TP3 and TP4, were driven under the approach embankment outside the footing at 17 ft (5.2 m), north of the abutment northernmost pile row and 10 ft (3.0 m) apart from one another. Pile TP4 was driven to the same depth as pile TP1. Pile TP3 was terminated 5 ft (1.5 m) higher (same as pile TP2).

4.2 Pile and soil instrumentation

All four piles were instrumented with vibrating wire (VW) strain gauges at intervals of approximately 4.5 m (15 ft). The lowest gauge levels, the 11th, in TP1 and TP4, and the tenth in TP2 and TP3, were at 42.1 m (138 ft) depth and 40.5 m (133 ft), respectively. The instrumentation did not include telltales.

To monitor the ground settlement, two settlement plates, stations 1 and 2 (Figure 4), were placed on the ground surface just outside the abutment footing at the centreline and at 13 m (40 ft) off the centreline. The settlement monitoring did not include measuring settlement distribution with depth; also the potential settlement of the abutment was not included in the monitoring schedule.

Two piezometer stations were placed at stations 1 and 2 with piezometer gauges in the clay at elev.+195.1, +189.0 and +182.9 m (elev.+640, +620 and +600 ft), that is at depths, labelled A, B and C, of 12.2, 18.3 and 24.4 m (40, 60 and 80 ft).

5. Results of new Eisenhower Bridge monitoring

5.1 Settlement and pore pressure

The settlement plates, piezometers and VW gauges were monitored from day 93. The monitoring ceased on day 895 because of

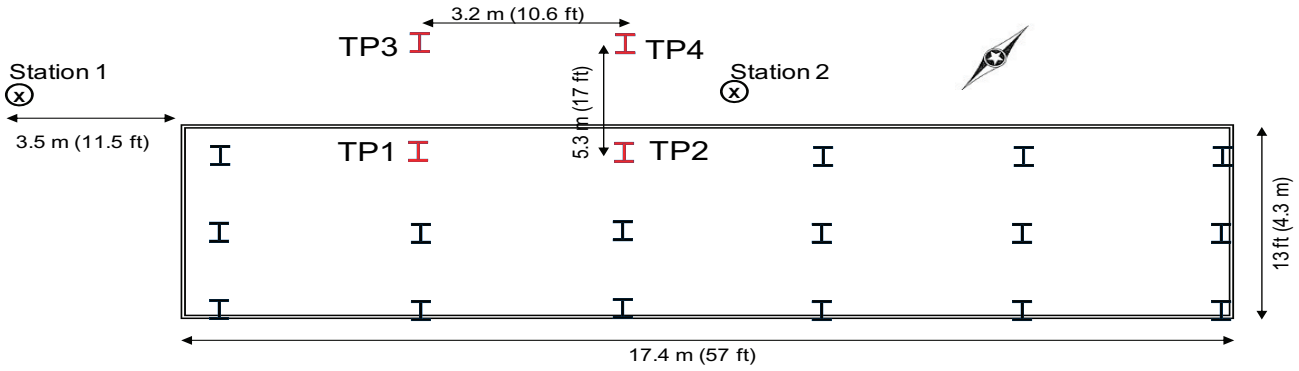


Figure 4. Abutment footing and pile plan with location of the outside piles

vandalism to the data collection unit. Based on the slowing rate, it appears most of the consolidation settlement was complete by about day 840 after about 3 m (10 ft) of surcharge had been removed. Figure 5 shows the measured ground settlement. It would seem that even with the wick drain acceleration, the consolidation settlement of the compressible soil required about a full year to develop (about days 430 through 840). Based on roadway maintenance reports, some minor settlement and tilting of the bridge approach panels was noticed when monitoring was terminated.

The pore pressure development in the piezometers is plotted in Figure 6. The piezometers reacted to the construction placement and removal of embankment fill, although not all such activities were documented. The last readings were taken exactly 3 years after the very first readings. There seemed to be an issue with the zero reading in Pz 1A, the upper piezometer gauge at station 1. It shows a very low pore pressure in relation to the readings at depths B and C. The readings at station 2 are more logical.

The readings during the first 3 months after the installation of the piezometers on 29 October 2017, day 95 were affected by construction activities and adding of fill. Figure 7 shows the change of pore pressure as different to the readings taken on day 1 (15 March 2018) at the two piezometer stations. The calendar dates for days 450, 643 and 890 are 20 October 2018, 1 May 2019 and 1 March 2020, respectively. The maximum pore pressure increase was about 40 kPa (6 psi), corresponding to the stress imposed by an approximately 2 m (7 ft) height of fill, as opposed to the 8 m (25 ft) height of the actually

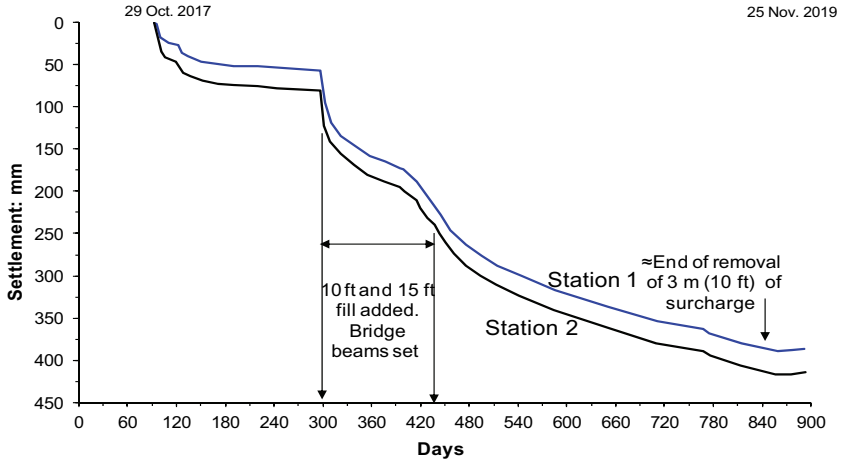


Figure 5. Measured ground settlement

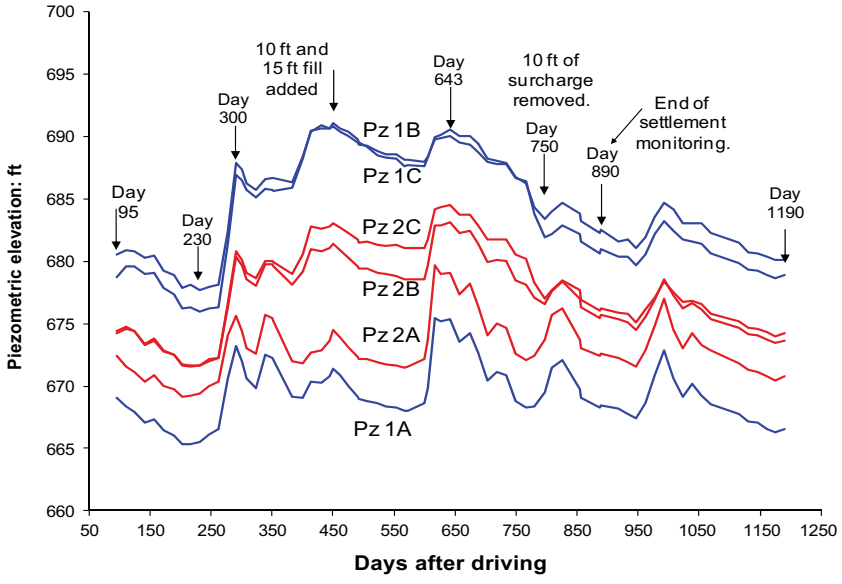


Figure 6. Measured pore pressures

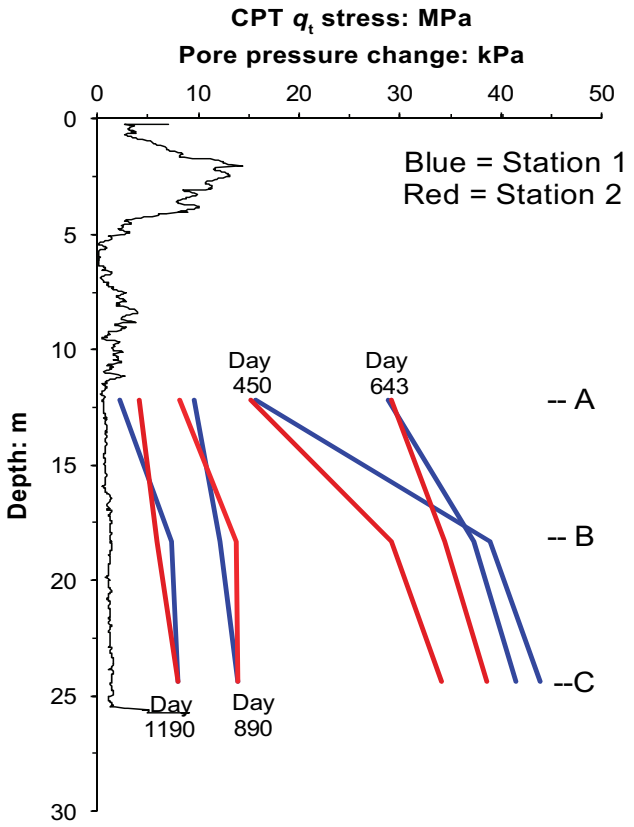


Figure 7. Change of pore pressure from day 1 to days 450, 643, 890 and 1190

placed embankment (not corrected for horizontal stress distribution with depth). Obviously, much of the induced pore pressure increase dissipated during the 2 years of construction time before the approach embankment reached full height (about day 640). As mentioned, the consolidation appeared to be completed by about day 840.

The very last set of readings (day 1190) shows about 3 to 8 kPa pore pressure larger than the 'zero reading', implying that not all induced pore pressures had dissipated. However, this is likely to be due to the fact that the piezometer tips settled with the soil (about 0.2 to 0.4 m corresponding to 2 to 4 kPa), thus registering the effect of the correspondingly larger distance up to the groundwater table. The seasonal difference (rise) in groundwater level in October (last reading) as opposed to the March 'zero reading' will have had a corresponding additional effect.

5.2 Strain and force in the piles

Starting 18 days after the pile driving, the strains in the VW gauges in the test piles were monitored at intervals ranging from 3 days to a month. Figures 8 and 9 show strain plotted against time with major construction events indicated. Piles TP1 and TP4 are the piles bearing on sandstone and piles TP2 and TP3 are the shallower piles bearing within the sand and gravel layer about 1.5 m (5 ft) above the sandstone. The strains reached a peak at about day 500, when the bridge deck was poured, and stayed approximately constant thereafter until the removal of 3.0 m of the surcharge. Two of the VW gauges in pile TP4 depths 42.1 m (138 ft) and 16.5 m (54 ft) ceased to function; an asterisk indicates their last record.

Figure 10 shows the distribution of strains in the piles terminating on sandstone (TP1 and TP3) and the piles terminating within the sand and gravel above the sandstone (TP2 and TP4), respectively. For TP1, the uppermost gauge level registered about 200 $\mu\varepsilon$, which, converted to force by multiplication with the EA parameter, correlates to about 1000 kN (200 kips). This is about equal to the designed abutment load. Interestingly, the strain in abutment pile TP2 registered less than the designed abutment pile load, which is likely to be due to its smaller toe resistance, resulting in the pile-head response becoming less stiff than for pile TP1 having a larger toe resistance. The maximum strain measured in the uppermost gauge level in piles TP3 and TP4 represented the same or larger load than the designed abutment load. That is, the pile head of the outside piles responded as an inverted pile-toe, registering 'toe' resistance in response to that equivalent 'toe penetration' (soil movement). The large values make sense considering the large downward movement (settlement) of the soil adjacent to and above the free pile head, that is movement ('penetration') relative to the pile head.

The maximum strain measured developed at the equilibrium plane (EP) and was about 600 $\mu\varepsilon$ in the two piles terminating in the sandstone and in pile TP3 outside the footing, which terminated in the sand and had the largest load at the pile head gauge. The 600 $\mu\varepsilon$ value correlates to about 127 MPa (18 ksi) stress. While large, this is still well below the yield strength of the H-pile.

In response to the soil settlement, all four test piles registered increasing axial strain (force) and build-up of toe resistance, developing a force equilibrium between the load at the pile head plus drag force versus accumulated positive shaft resistance and toe resistance. The length, or height, of the zone showing the transition from negative direction shaft resistance to positive direction is about 10 to 15 m (30 to 45 ft) The toe resistance in the deeper piles bearing on the stiffer sandstone was considerably larger than for the shallower piles and their equilibrium plane was, therefore, located at greater depth.

Recently, a revised approach of the American Association of State Highway and Transportation Officials (AASHTO) specifications was published in a National Cooperative Highway Research Program (NCHRP) report (Coffman *et al.*, 2024b) detailing the design analysis for a piled foundation subjected to area settlement (general subsidence), such as for the subject foundation. The approach, which is expected to be incorporated in the next edition of the AASHTO specifications, was built on the unified method (Fellenius, 1984, 1988, 2004, 2026), which combines force and settlement distributions: (*a*) the distribution of long-term force

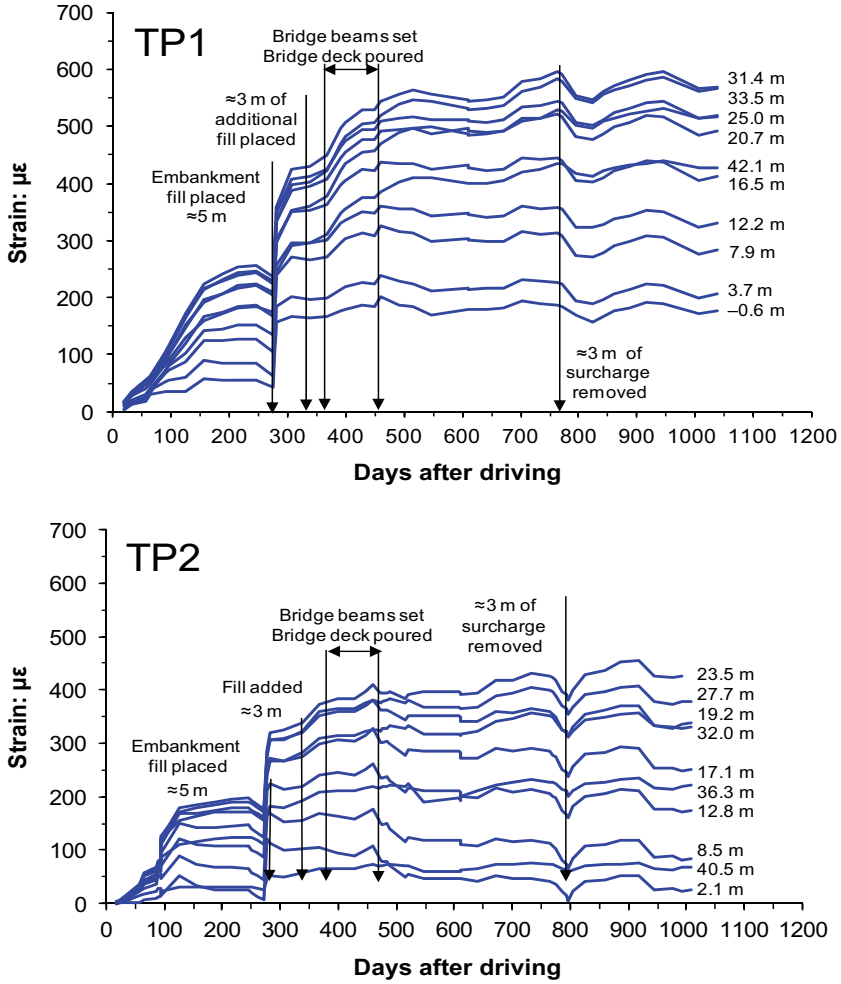


Figure 8. Axial strain plotted against time (days) in the abutment foundation piles, piles TP1 and TP2

developed due to applied sustained load and accumulated negative skin friction due to downdrag with (*b*) the distribution of long-term soil and pile settlements (pile-toe movement and compression). The distributions in the two graphs (Figure 11) are independent. However, the pile-toe force in the force distribution graph and the pile-toe movement in the settlement distribution graph are interrelated by the pile-toe force–movement expressed in a *q*–*z* function (Fellenius, 2025). The shaft resistance is, similarly, expressed in a *t*–*z* function. Usually, after an initial movement, the pile–soil shaft interaction can be assumed to follow an almost plastic shear response, making the shaft resistance (*t*–*z* function) less controlling for the graph curves than the toe resistance (*q*–*z* function).

Figure 11 shows, for pile TP1, graphs of force and settlement distributions according to the unified method. The curve 'Fitted by UniPile' in Figure 11(a) was produced by means of the UniPile6 software (UnisoftGS.com). It shows the fit to the day 1007 distribution in an effective stress analysis. Only the settlement of the upper surface of the embankment (ground) was measured. In Figure 11(b), the 'Soil' curve shows the distribution of soil settlement starting at the values measured at the ground and calculated using UniPile. The 'Pile' curve shows the pile settlement, starting at the toe penetration and increasing up to the abutment by pile compression due to the axial force. The term r_s/σ' in Figure 11(c) indicates the β-coefficient for the fitted force distribution (r_s is the unit shaft resistance and σ' is the effective stress).

The calculation applies the Boussinesq distribution for the stress due to the approach embankment and the stated compressibility of the clay. The input of compressibility of the sand layers was fitted to the measured settlement. The pile-toe penetration due to the toe force was estimated from the strain-determined axial compressions and fitted *q*–*z* curves to have been about 20 mm or smaller. The value at the pile head is the pile settlement due to applied load and downdrag.

Pile TP1 developed an equilibrium plane at a depth of about 31 m in the sand. Figure 11(c) shows that the transition from negative

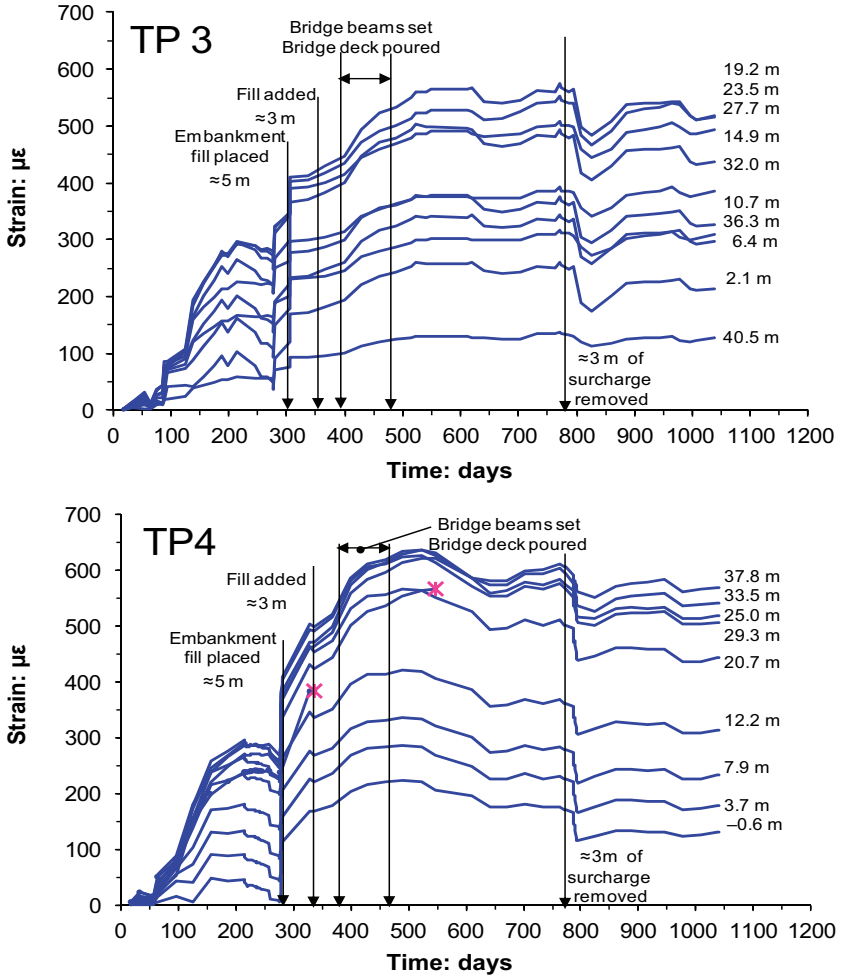


Figure 9. Axial strain plotted against time (days) in the external embankment piles, piles TP3 and TP4

skin friction to positive shaft resistance developed between the depths of approximately 23 and 33 m. On day 1007, the drag force taken as the increase of axial force (converted from strain) at the equilibrium plane was about 1500 kN.

If assuming that the shear pile-to-soil occurred along the 1.4 m^2/m rectangular circumferential pile area, the values correlate to an average unit shaft resistances of about 40 kPa, both above and below the transition zone. However, shaft resistance is a function of effective stress. The ratio between the unit shaft resistance and the effective stress, r_s/σ', is shown in Figure 11(c). The ratio is constant in the upper sand layer, reducing in the clay as the relative movement between the pile and the soil decreases, reaching zero at the EP, where no relative movement occurs, and it then increases with distance from the EP due to increasing relative movement. The ratios would seem to correlate well with movement, but, because the movement is not measured but estimated, and the movement range is large, correlating the ratio directly to the movement would have little value.

Figure 12 compiles the r_s/σ', ratio for the four test piles. All four showed a constant ratio in the loose sand, indicating a plastic response. In contrast, the shaft resistance response in the silty clay is significantly affected by the relative movement between the pile and the soil, that is, it is strain-hardening, which also appears to be the case in the lower sand layer, The EP for the piles terminating in the sandstone was at about 31 m(100 ft) depth, while it was at about 23 m (75 ft) depth for the piles terminating in the sand layer. For the latter, the higher EP level means that had the foundation piles been installed to terminate in the sand as opposed to in the sandstone, considering their larger toe movement, the foundation would have settled about 100 mm (4 in) due to downdrag.

6. Conclusions

The records of the old 1960 Eisenhower Bridge showed that the drag force had exceeded the structural strength of the wood piles, which effectively removed pile bearing and caused the piles to be dragged down by the long-term soil settlement.

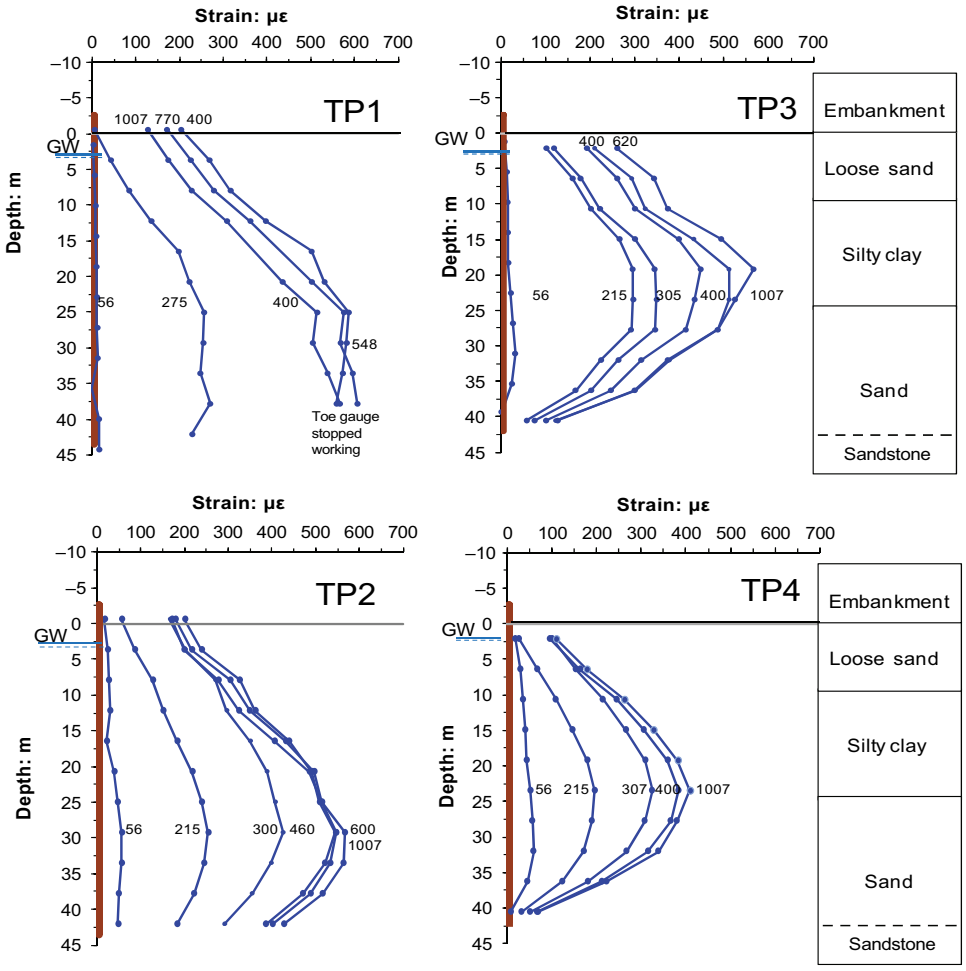


Figure 10. Axial strain plotted against depth at selected times (days)

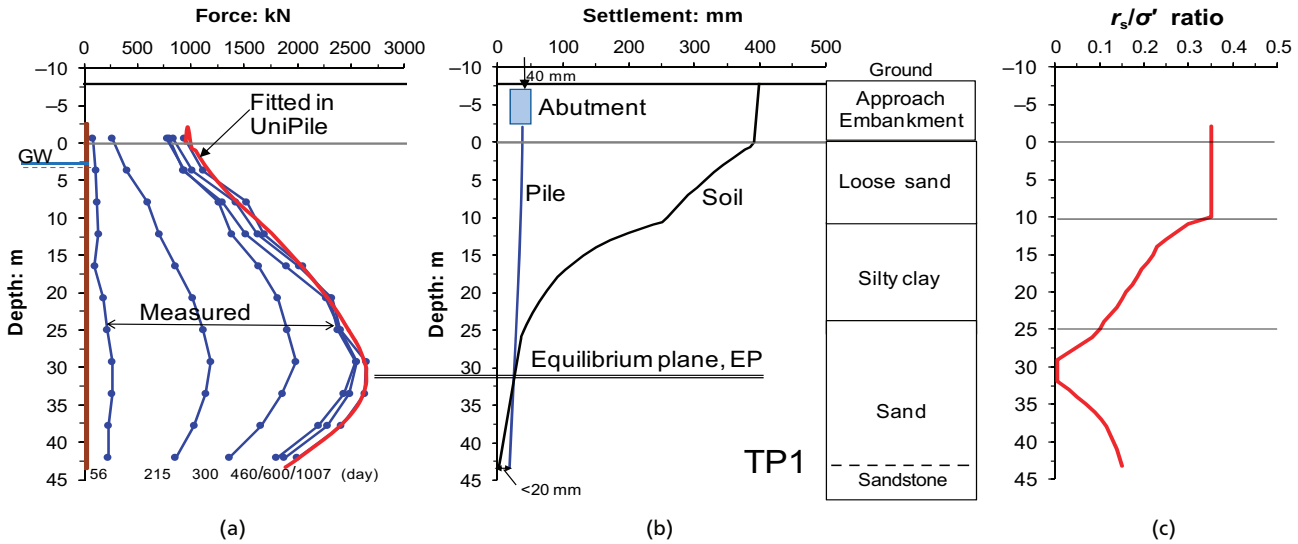


Figure 11. Pile TP1: Distributions of force (a), settlement (b) and back-analysis r_s/σ' ratio (c) according to the unified method

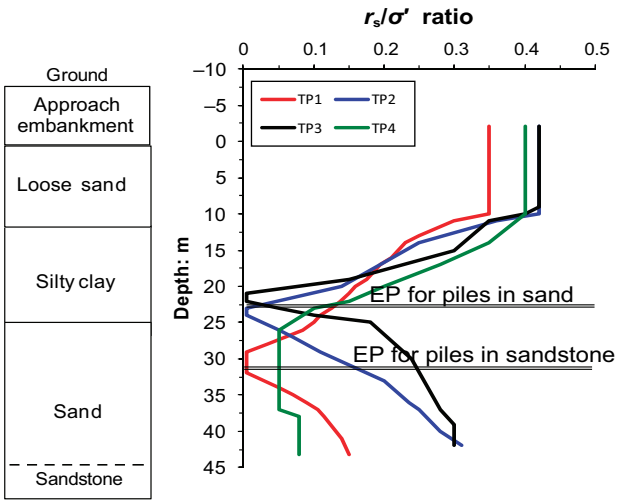


Figure 12. Compilation of r_s/σ' ratios

The monitoring of the replacement Eisenhower Bridge north abutment, which was supported on steel H-piles, showed similar behavioural trends as seen in earlier Minnesota Department of Transportation (MnDOT) performance monitoring projects, including the accumulation of drag force as approach embankments were placed, loading the soils and triggering consolidation settlement. An equilibrium plane developed early during construction and remained at a relatively fixed elevation during the course of construction and application of service loads.

This project afforded a rare opportunity to examine and compare the behaviour of four driven piles, with different toe bearing conditions, in an environment where the anticipated drag force influence was large. Two instrumented test piles were located within the abutment foundation footprint, one driven into the sandstone and one terminated about 5 ft (1.5 m) in sand above the sandstone. Two additional instrumented test piles were driven within the newly placed backfill outside the abutment footing to the same length and toe conditions.

The equilibrium plane of the construction piles was at about 30 ft (10 m). It was slightly deeper for the test piles extending to the sandstone compared to the slightly shorter piles that terminated in the sand. The construction pile terminating in the sand was shown to carry smaller load than the pile terminating in the sandstone. This is an effect of the latter being stiffer and, therefore, absorbing more load to ensure equal pile-head movement.

The piles under the embankment not connected to the bridge were shown to carry as much or larger load than the foundation piles. The load was caused by the embankment soil moving down around the pile, mobilising an upward 'toe' resistance at the free pile head, and the condition can be regarded as the pile carrying the weight of an inverted cone of embankment fill on the pile head.

The downdrag for the embankment piles bearing in the sandstone was about 40 mm (1.6 in), while the piles bearing in the sand experienced about 100 mm (4 in) downdrag.

While sometimes complex, due to construction staging and geometry, the pile strain and the soil pore water pressure response appeared to agree well with the observed soil fill placement and loading. The results over the 3 years of monitoring indicated that the pore pressure dissipation (consolidation) required at least around 200 days to a year.

The approach embankment settled about 400 mm (16 in), while the monitored piles settled only due to elastic compression and a small toe penetration. The abutment foundation production piles are estimated to have settled about 40 mm (1.6 in).

Observations showed that the wick drains were effective in accelerating consolidation and, therefore, reduced future long-term settlement and the associated need for maintenance after the roadway was open to traffic.

The measured response of the test piles was in excellent agreement with the principles of the unified method and could be back-calculated according to the shaft and toe resistance based on effective stress analysis employing the UniPile6 software.

The maximum axial force in the pile, consisting of sustained load and drag force, was well within the limits of the pile's structural strength.

REFERENCES

Bartz JR and Blatz JA (2020) Comparison of Canadian highway bridge design code and AASHTO LRFD bridge design specifications regarding pile design subject to negative skin friction. *Canadian Geotechnical Journal* **57(7)**: 1092–1098, 10.1139/cgj-2019-0247.

Bjerrum L, Johannessen IJ and Eide O (1969) Reduction of negative skin friction on steel piles to rock. *Proceedings of the 7th ICSMFE*, Mexico City, vol. 2, pp. 27–33.

Coffman RA, Blanchard JD, Stuedlein AW, Jana A and Budge AS (2024a) *Design of Piles for Downdrag.* TRB, Washington, DC, USA, p. 353.

Coffman RA, Stuedlein A and Budge AS (2024b) *Pile Design for Downdrag – Examples and Supporting Material*. TRB, Washington, DC, USA, p. 285.

Dasenbrock DD, Chow LC and van Heuven DS (2021) Evolution of the dragload behavior during construction of four H-piles with different top load and end fixity conditions at a bridge abutment with embankment fill, p. 16

Dasenbrock DD and Chow LC (2023) Comparing downdrag design: Eisenhower Bridge of Valor. *University of Minnesota 71st Annual Geotechnical Engineering Conference*, p. 13.

Endo M, Minou A, Kawasaki T and Shibata T (1969) Negative skin friction acting on steel piles in clay. *Proeedings of the 7th ICSMFE*, Mexico City, vol. 2, pp. 85–92.

Fellenius BH and Broms BB (1969) Negative skin friction for long piles driven in clay. *Proceedings of the 7th International Conference on Soil Mechanics and Foundation Engineering*, Mexico City, vol. 2, pp. 93–97.

Fellenius BH (1984) Negative skin friction and settlement of piles. *Proceedings of the Second International Seminar on Pile Foundations*. Nanyang Technological Institute, Singapore, pp. 28–30.

Fellenius BH (1988) *Unified Design of Piles and Pile Groups*. Transportation Research Board, Washington, DC, USA, pp. 75–82.

Fellenius BH (2004) Unified design of piled foundations with emphasis on settlement analysis. *Honoring George G. Goble Current Practice and Future Trends in Deep Foundations. Geo-Institute Geo-TRANS Conference*, Los Angeles, CA, USA (DiMaggio JA and Hussein MH (eds)), **125**, pp. 253–275. American Society of Civil Engineers, Reston, VA, USA.

Fellenius BH (2006) Results from long-term measurement in piles of drag load and downdrag. *Canadian Geotechnical Journal* **43(4)**: 409–430.

Fellenius BH (2026) Basics of foundation design – a textbook, electronic edn. See www.Fellenius.net (accessed 05/06/2026).

Johannessen IJ and Bjerrum L (1965) Measurements of the compression of a steel pile to rock due to settlement of the surrounding clay. *Proceedings of the 6th ICSMFE*, Montreal, Canada, vol. 6, pp. 261–264.

Okabe T (1977) Large negative friction and friction-free piles methods. *Proceedings of the 9th ICSMFE*, Tokyo, Japan, vol. 1, pp. 679–682.

Olson SJ (2020) Eisenhower Bridge north abutment and approach settlement: a case history of timber pile downdrag and comparative downdrag effect on steel piles. In *Geo-Congress 2020: University of Minnesota 68th Annual Geotechnical Engineering Conference* (Labuz JF, Theroux BA, Hambleton JP, Makhnenko R and Budge AS (eds)). American Society of Civil Engineers, Reston, VA, USA, Geotechnical Special Publication GSP **321**.

Siegel TC (2025) Drag load: the geotechnical boogeyman. *GEOSTRATA Magazine* **27(3)**: 14–15.